
Three-directional grating and application in measuring residual stresses

JuBing Chen

Engineering Mechanics Department, Shanghai Jiaotong University, 200240 Shanghai, PR China

E-mail: jbchen@mail.sjtu.edu.cn

Abstract The performance of mechanical parts is influenced by residual stresses on grinding surfaces. Because of the randomness of residual stresses, they are very difficult to determine by theory. A three-directional grating is presented by the author, and by means of the moiré interference technique and hole-drilling, a new method of residual stress measurement is developed. Further, the residual stresses on grinding surfaces are given.

Keywords residual stresses; three-directional grating; grinding; measuring

There are many research works on the measurement of residual stress. Techniques include the X-ray diffraction method [1], holography [2], crossed grating moiré interference technique [3], speckle interferometer [4], hole-drilling strain gauges method [5], ultrasonic methods [1], and magnetic methods [1]. Each technique has advantages for particular problems, as well as disadvantages. For example, with the hole-drilling strain gauges method, the strains always are averaged in the area of the strain gauge; with the holographic technique and speckle interferometer, the problems are how to review and reconstruct the fringes with high accuracy in order to determine the strains.

In this paper, a three-directional grating is presented, which, by means of the moiré interference technique and hole-drilling, can measure the residual stress on a grinding surface. It should be stressed that in moiré interferometry one-directional or crossed gratings are generally applied. In crossed grating moiré interferometry, two fringe patterns can be obtained to determine the full strain evaluation (ε_1 , ε_2 and γ_{xy}), but for measuring residual stress, when a hole is drilled to relax it, the specimen must move, and it is very difficult to reposition it with high precision; there must therefore be errors when comparing the corresponding moiré patterns (before and after drilling) to determine the full strain evaluation. Especially when computing γ_{xy} from the derivatives of two fringe patterns, a very small rotation of the specimen may result in sizable errors. In contrast, with a three-directional grating and moiré interferometry, three fringe patterns can be obtained to determine the full strain evaluation (ε_1 , ε_2 and ε_3), and the specimen can be repositioned accurately after drilling; the errors become less than in crossed grating moiré interferometry, and as the fringe change is always measured along the normal direction, this can reduce errors also.

Principles of measurement

The residual stresses on a grinding surface relax when a hole is drilled on the surface. They can be determined by detecting this release, which is expressed by deforma-

tion of the grinding surfaces. To measure the deformation, a three-directional grating and moiré interferometry are applied. The directions of this kind of grating are set at 0° , 45° and 90° , and the corresponding moiré patterns in each direction can be obtained before and after drilling hole. We compare the corresponding moiré patterns before and after drilling. The three strain components, ε_0 , ε_{45} and ε_{90} , can be computed [6]:

$$\varepsilon_x = \frac{\partial U}{\partial x} = \frac{1}{2f} \left[\frac{\partial N_x}{\partial x} \right] = \frac{1}{2f} \left[\frac{N_{x2} - N_{x1}}{\Delta x} \right] \quad (1)$$

Where ε_x is the normal strain along x , x denotes the 0° , 45° and 90° direction, f is the frequency of grating ($f = 1000$ lines/mm), Δx is a small displace unit, N_{x1} , N_{x2} are the numbers of moiré fringes in Δx before and after drilling the hole. The principal strains, ε_1 and ε_2 , can be computed according to following equations [7]:

$$\varepsilon_1 = \frac{1}{2} \left[\varepsilon_0 + \varepsilon_{90} + \sqrt{2} \sqrt{(\varepsilon_0 - \varepsilon_{45})^2 + (\varepsilon_{45} - \varepsilon_{90})^2} \right] \quad (2)$$

$$\varepsilon_2 = \frac{1}{2} \left[\varepsilon_0 + \varepsilon_{90} - \sqrt{2} \sqrt{(\varepsilon_0 - \varepsilon_{45})^2 + (\varepsilon_{45} - \varepsilon_{90})^2} \right] \quad (3)$$

$$\text{tg}2\theta_0 = -\frac{2\varepsilon_{45} - (\varepsilon_0 + \varepsilon_{90})}{\varepsilon_0 - \varepsilon_{90}} \quad (4)$$

where θ_0 is the angle measured counter-clockwise from the direction of 0° grating to the direction of ε_1 . The stresses can be calculated from the measured strains, according to Hooke's law [8]:

$$\sigma_1 = \frac{E}{1-\nu^2} (\varepsilon_1 + \nu\varepsilon_2) \quad (5)$$

$$\sigma_2 = \frac{E}{1-\nu^2} (\varepsilon_2 + \nu\varepsilon_1) \quad (6)$$

where E is the elastic modulus and ν is Poisson's ratio.

Experimental procedure

Manufacture of the three-directional grating

The optical set-up used to manufacture the three-directional master grating is shown in Fig. 1. Based on the power of the incident beams and the type of holographic plate used, the proper exposure time should be determined first. Then, a first exposure is made. The holographic plate is then rotated 90° and 45° , and a second and third exposure are made after each rotation. Finally, the holographic plate is developed, fixed, bleached and coated with gold, producing a three-directional master grating.

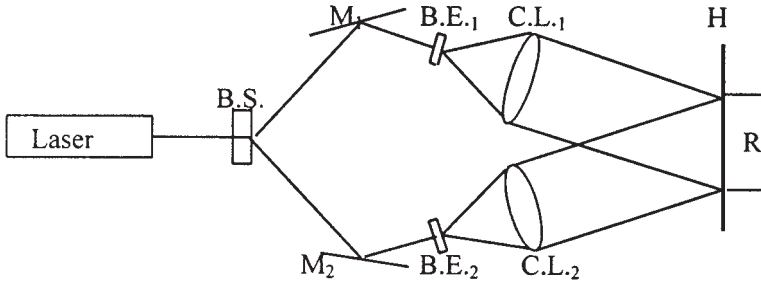


Fig. 1 Experimental set-up for the manufacture of the three-directional grating. B.S., beam splitter; B.E.₁, B.E.₂, beam expanders; M₁, M₂, mirrors; C.L.₁, C.L.₂, collimate lenses; H, hologram; R, rotatable stage.

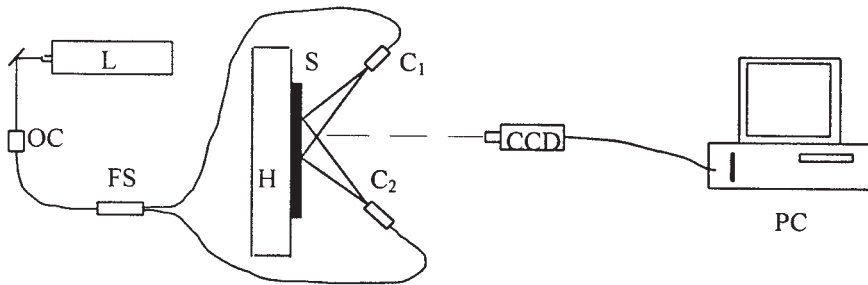


Fig. 2 Experimental set-up for measuring residual stresses. L, laser; OC, optical coupler; FS, Y-optical fibre; C₁, C₂, chucks; S, specimen; H, rotatable worktable; CCD, video camera; PC, personal computer.

The measurement of residual stresses

The specimens were installed on the rotatable worktable; the specimens measured 160 mm × 18 mm × 6 mm. A 1000 lines/mm three-directional grating was transferred onto the surface of the specimen. It was replicated from the master grating produced earlier.

Fig. 2 shows the experimental set-up. The laser beam is linked to a polarization-preserving fibre optic coupler with a coupling ratio of 50%, such that the same light power is delivered to the two branches. Those two laser beams illuminate the surface of the specimen on which the grating is bonded and act as the reference grating. The two superposed gratings give the moiré fringe system in the first direction (for example the *x*-axis) (Fig. 3a), which is sent from the CCD camera to a personal computer. The specimen is rotated 90° and 45°, respectively, and the process above is repeated; thus the moiré fringe systems in the other two directions (*y*-axis, and the bisector between the *x*-axis and *y*-axis) (Fig. 3e, 3c) are obtained. Then the specimen is taken off the rotatable worktable, and a hole (radius $a = 1.0$ mm; depth

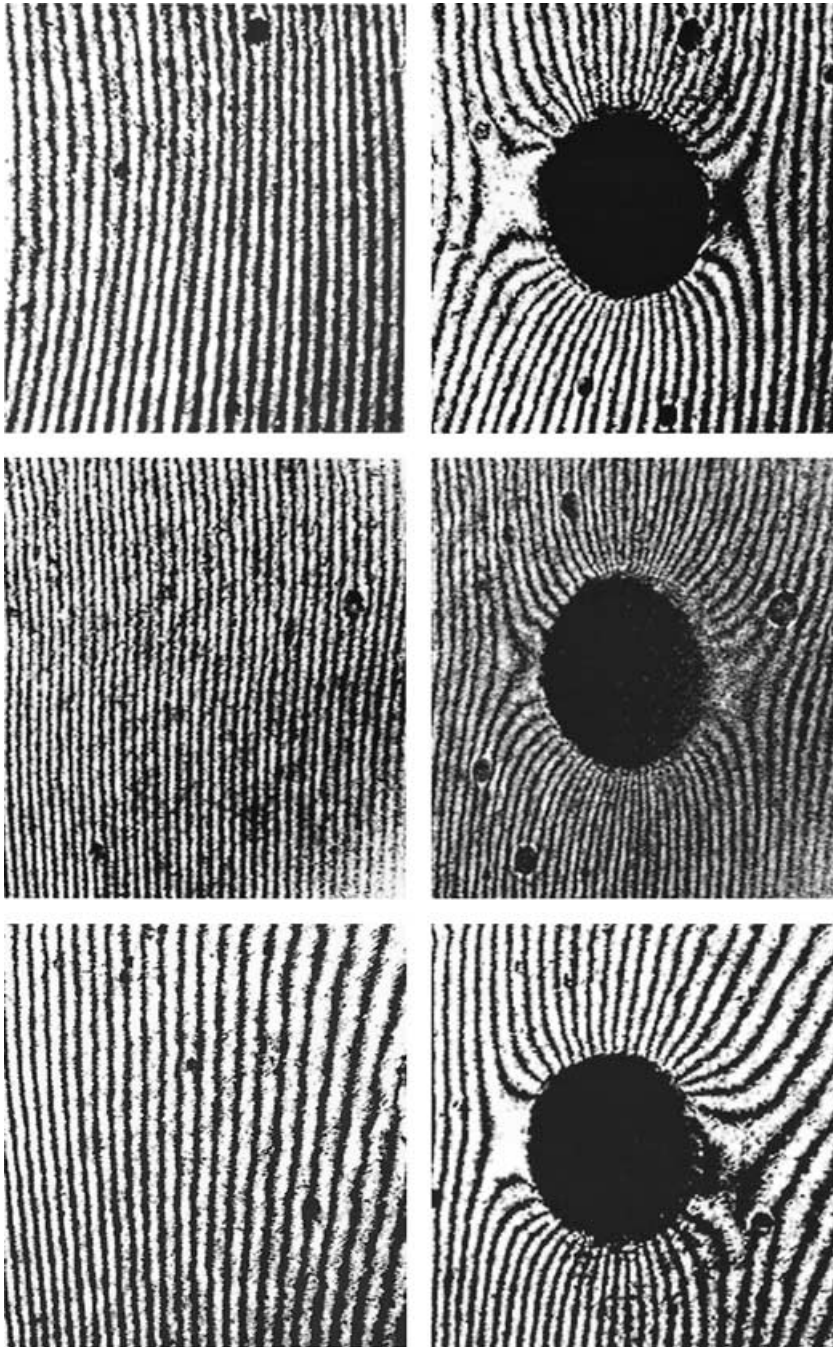


Fig. 3 *Moiré images before drilling hole (the left column) and after drilling hole (the right column).*

$h = 1.0 \text{ mm}$) is drilled on the surface of the specimen on which the grating is bonded. In order to reinstall the specimen accurately in the same position on the rotatable worktable, we can locate it by the moiré pattern, because the fringes on the edge of moiré pattern change little if the moiré pattern is large enough. The corresponding three-direction (x , y -axis, and the bisector) moiré fringe systems (Fig. 3b, 3f, 3d) are obtained. By comparing the fringe systems before drilling with after drilling (i.e. Fig. 3a with 3b, Fig. 3c with 3d, and Fig. 3e with 3f), the residual strains can be computed by determining the change of fringe pitch. From this the residual stresses can be calculated [8].

Calibration

Fig. 4 represents an aluminium calibration specimen. Before drilling the hole, the aluminium calibration specimen is restricted with a frame, which is much stiffer than the specimen. A uniform tension was applied in the x direction ($\varepsilon = 903 \mu\varepsilon$), and fixed in the frame. After the strain was almost steady (the movement of strain is no more than $3 \sim 3 \mu\varepsilon$ in two hours), it was regarded as ready for testing. The specimens measured $160 \text{ mm} \times 18 \text{ mm} \times 6 \text{ mm}$.

The experimental data for the aluminium specimen were obtained using the moiré interferometry system described earlier. The calculational data were computed using the following equations [8]:

$$\sigma_r = \frac{S}{2} \left(1 - \frac{a^2}{r^2} \right) + \frac{S}{2} \left(1 + \frac{3a^4}{r^4} - \frac{4a^2}{r^2} \right) \cos 2\theta \quad (7)$$

$$\sigma_\theta = \frac{S}{2} \left(1 + \frac{a^2}{r^2} \right) - \frac{S}{2} \left(1 + \frac{3a^4}{r^4} \right) \cos 2\theta \quad (8)$$

$$\tau_{r\theta} = -\frac{S}{2} \left(1 - \frac{3a^4}{r^4} + \frac{2a^2}{r^2} \right) \sin 2\theta \quad (9)$$

where a is the radius of the drilling hole, S is the uniform tension applied to the specimen as shown in Fig. 4 (the relations between the components of stresses and the components of strains are determined by Hooke's law), r is a distance from the

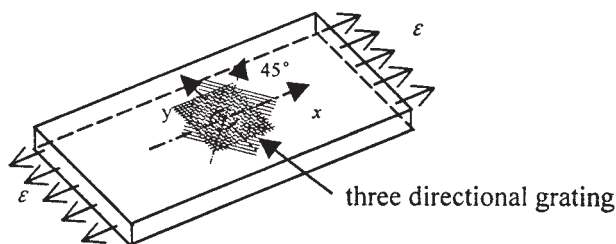


Fig. 4 Specimen geometry and grating position.

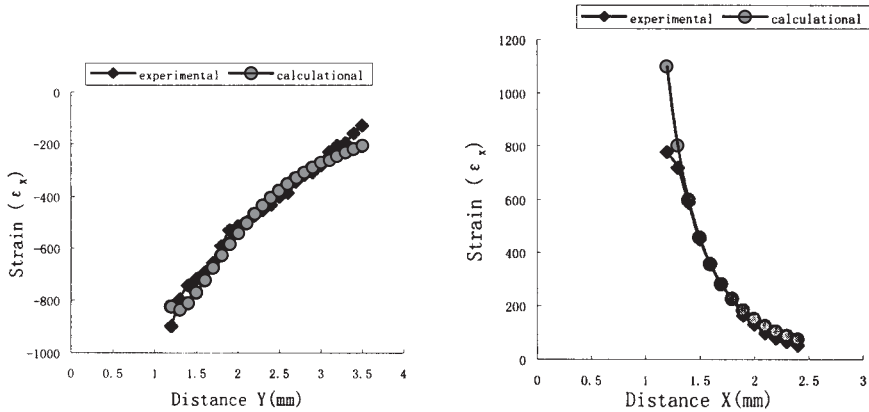


Fig. 5 Comparison of experimental data with calculational data.

point to the centre of the drilling hole, θ is the angle measured counter-clockwise from the x -axis to the radial which is from the point to the centre of the drilling hole.

We computed the results for $\theta = 0^\circ$, 45° and 90° , and they are compared in Fig. 5. There was good agreement between the experimental data and the calculational data (the maximum relative error is no more than 15%). Therefore this method is suitable for testing residual stresses.

The testing of residual stresses on a grinding surface

The residual stresses on grinding surfaces are very complicated, as they are affected by many factors, especially those factors which cause plastic deformation, heating or thermochemical treatment. Radial feed (f_r) is considered to have a large influence on the average temperature in the grinding zone (θ_{av}), and θ_{av} has a large influence on plastic deformation, heat stress, phase transition, and thermochemical treatment. For this reason, radial feed (f_r) was selected as the main factor causing residual stresses on the grinding surface.

The specimen geometry and grating position were as shown in Fig. 4. The specimen's size was $160 \times 18 \times 6 \text{ mm}^3$. It was made out of steel (45, homogenization treatment) and had an elastic modulus of 200 GPa and a Poisson ratio of 0.3. The grinding wheel was GB45ZR10A $300 \text{ mm} \times 30 \text{ mm} \times 75 \text{ mm}$. The surface speed of the grinding wheel (v_s) was 30 m/s. The speed of the workpiece (v_w) was 0.15 m/s. The radial feeds used were $f_r = 0.015, 0.020, 0.025, 0.030, 0.035, 0.040, 0.045, 0.050, 0.055 \text{ mm}$.

It was assumed that this mechanics question could be regarded as a plane question, because the depth of specimen and the depth reached by residual stresses are much smaller than the length or width, and when the depth of hole is more than 1.0 mm there is little relaxation of residual stresses in measuring. It was also assumed that the specimen material is isotropic.

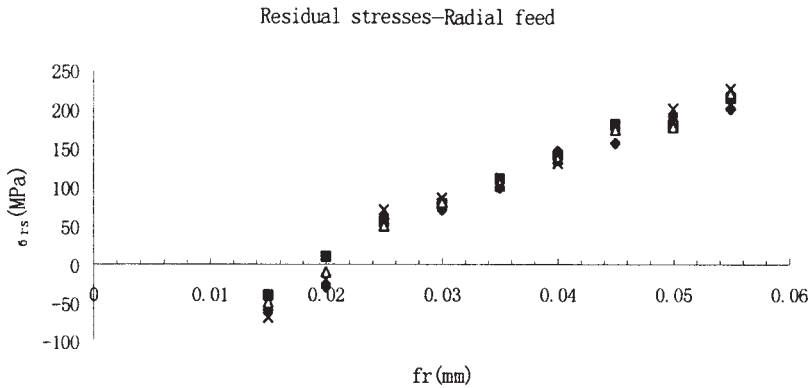


Fig. 6 Residual stresses – Radial feed.

The results are show in Fig. 6.

Conclusions

- (1) The manufacture of a three-directional grating by the interference technique is feasible.
- (2) The measurement of residual stresses by means of a three-directional grating and moiré interferometry gives results that are accurate – the maximum relative error is no more than 15%.
- (3) The magnitude of residual stresses (σ_{rs}) on a grinding surface will increase with radial feed (f_r), and it forms tension stress as the radial feed (f_r) increases.

References

- [1] J. Lu, *Handbook of Measurement of Residual Stresses* (Fairmont Press, India, 1996), 5–30.
- [2] A. Makino and D. V. Nelson, ‘Determination of subsurface distributions of residual stress by a holographic hole-drilling technique’, *J. Eng. Tech.*, **119**(1) (1997), 95–103.
- [3] S. P. He, E. Guan, Y. S. Shu, X. P. Wu, ‘Applying moiré interference technique determining distributions of residual stress’, *Acta Mechanica Sinica*, **25**(4) (1993), 485 (in Chinese).
- [4] D. R. Schmitt and R. W. Hunt, ‘Inversion of speckle interferometer fringes for hole-drilling residual stress determinations’, *Exp. Mech.*, **40** (2000), 129.
- [5] H. L. Pang and S. R. Punas, ‘Residual stress measurements in a cruciform welded joint using hole drilling and strain gages’, *Strain*, **25**(1) (Feb. 1989), 7–14.
- [6] D. Post, B. Han and P. Ifju, *High Sensitivity Moiré* (Springer-Verlag, New York, 1994), 114–130.
- [7] H. W. Liu, *Material Mechanics* (Education Press, Beijing, 1992) (in Chinese), 208–210.
- [8] S. P. Timoshenko, *Theory of Elasticity* (McGraw-Hill Book Company, Auckland, 1991), 8–12, 90–96.